Advanced Composite Materials
Publication details, including instructions for authors and subscription information:
http://www.tandfonline.com/loi/tacm20

Bonding strength of SiC coating on the surfaces of C/C composites

Hiroshi Hatta , Yoshifumi Nakayama & Yasuo Kogo

Version of record first published: 02 Apr 2012.

To cite this article: Hiroshi Hatta , Yoshifumi Nakayama & Yasuo Kogo (2004): Bonding strength of SiC coating on the surfaces of C/C composites, Advanced Composite Materials, 13:2, 141-156

To link to this article: http://dx.doi.org/10.1163/1568551041718035

Adv. Composite Mater., Vol. 13, No. 2, pp. 141–156 (2004)

Also available online - www.vsppub.com

Bonding strength of SiC coating on the surfaces of C/C composites

HIROSHI HATTA [1,*], YOSHIFUMI NAKAYAMA [2] and YASUO KOGO [2]

[1] *The Institute of Space and Astronautical Science, Japan Aerospace Exploration agency, 3-1-1 Yoshinodai, Sagamihara 229-8510, Japan*
[2] *Department of Material Science and Technology, Science University of Tokyo, 2641, Yamazaki, Noda-shi, Chiba-ken 278-8510, Japan*

Received 10 October 2003; accepted 16 March 2004

Abstract—Carbon fiber-reinforced carbon matrix composites (C/Cs) are usually used with an anti-oxidation coating. For the prevention of exfoliation, high strength bonding of the coating to the C/C substrate is often required. However, no measures have been established to determine bonding strength for thin and brittle coatings. In the present paper, first, a criterion for interfacial fracture of a SiC coating on a C/C substrate was discussed on the basis of fracture loads measured by a specially designed plunger method. The fracture mechanics approach was shown to be successful to predict the interfacial debonding. Then, a parametric study was carried out to understand the effect of various parameters on the interfacial fracture loads.

Keywords: SiC coating; C/C composite; interfacial bonding; conversion; fracture toughness.

1. INTRODUCTION

Carbon/carbon composites (C/Cs) are attractive materials for applications in high temperature structures because of their exceptional high temperature capability exceeding 2000°C [1, 2]. However, C/Cs possess serious deficits, the most serious of which is their weakness against high temperature oxidation [3]. Thus, countermeasures against C/C oxidation are an active topic in the C/C research community. Presently, the most promising measure is ceramic coating deposited on the surface of C/Cs. For example, SiC coatings are used at the nose cone and the leading edges of space shuttles. The principal requirements for the coating material are oxidation resistance, a low evaporation rate, chemical and mechanical compatibility with the substrate, and high adhesive strength of the interface between the C/C and coating.

*To whom correspondence should be addressed. E-mail: hatta@pub.isas.jaxa.jp

Currently, SiC is regarded as the most promising candidate to meet these requirements [4].

In actual application, mechanical loads exerted on the coating are often severe. For example, in turbine disks of space planes, high values of tensile and shear stresses may be induced onto the coating interface by centrifugal force and thermal shock. Thus, delamination of the coating often becomes a serious problem. However, no quantitative measures have been established to evaluate the adhesive strength of the coating to the substrate.

So far, four methods have been proposed for the evaluation of the bonding strength of hard and brittle coatings like SiC [5–7]. Standard techniques ordinarily used for the evaluation of adhesives, a single or double lap-shear method, might be applicable. In these methods, a substrate is bonded on the coated material, and tensile or shear stress is applied by gripping the two substrates. Precise evaluation is, however, difficult by these methods, when the bonding of the coating and the original substrate is strong. For such a case, fracture is prone to occur on the newly bonded interface or within the substrate. In addition, a specimen with a large size is usually required for these methods. The second method for the evaluation of the bonding strength is the scratch test. This technique is easy to perform and requires only a small sample. However, because of the complex fracture induced by this method, the values obtained are only useful for the comparison of the bonding strength among samples with the same configuration. For the quantitative determination of the bonding strength, Nakasa *et al.* [8–10] have proposed a method in which tensile force is applied to a coated specimen. In this method, the debonding load can be determined only when tensile strain of the substrate is much higher than that of the coating. When the substrate is brittle, as in case of C/Cs, then it will fracture first. Thus, this method is not convenient for coated C/C composites. Evans *et al.* [11–13] have proposed an indentation method. In this method, interfacial delamination occurs due to a compressive force applied by a Vickers indenter, and the energy release rate is then calculated from the delamination load. However, this method is difficult to apply in the present situation. A tensile thermal stress in the coating due to the mismatch of the thermal expansion between the coating and the thermal stress prevents delamination.

In the present paper, a newly designed plunger method will be proposed. In this method, shear force is directly applied to the coating interface, and thus the interface of a SiC coating deposited on a C/C composite can be fractured. Then, based on the experimental results, the critical energy release rates of the coating interface are determined using the finite element method. Finally, the interfacial fracture under various coating configurations and processing conditions is predicted on the basis of the predetermined critical energy release rates. These calculated results are compared with experimental observations.

2. EXPERIMENTAL

2.1. Materials

Two types of C/C composites, unidirectionally reinforced (UD) and cross-ply laminated (CP) C/Cs, were used in this study. These C/Cs were fabricated by the preformed yarn method [14], and supplied by Across Co. The reinforcing fibers of the C/Cs were high modulus type Torayca M40, their nominal volume fraction was 50%, and heat treatment temperature was 2000°C.

The SiC coating was composed of a conversion layer and a chemical vapor deposition (CVD) layer. The conversion layer was formed by the reaction between gas phase Si and carbon in the substrate C/Cs. The thickness of this layer was several μm and its aim was to relax the thermal mismatch stresses in the CVD layer and, by that, to improve its interfacial bonding. The conversion process time was varied from 0 to 10 hours to examine the effect of the conversion treatment time on the interfacial strength. Over the conversion layer, a dense SiC layer with a thickness of 50 to 180 μm was deposited by CVD at temperatures of 1200 or 1600°C. The details of the CVD process conditions have been given in previous papers [15, 16]. This two-layer coating was formed on only one side of the substrate. Before the coating treatment, the surfaces of the substrate C/Cs were polished by diamond paste with a powder diameter gradually decreasing from 15 to 1 μm.

Substrate C/Cs were provided by plates of 300 × 300 × 3.2 mm. The SiC coating was applied to substrates of 30 × 30 × 3.2 mm plates cut from the original plates. After the coating treatment, bonding test specimens were carefully cut into an individual size using a low speed and low load diamond wheel.

2.2. Definition of the specimen configuration

The bonding strength of the SiC coating may vary depending on the substrate C/Cs and the fiber orientation beneath the coating. To identify the surfaces and the loading directions, notations and Cartesian coordinate systems were defined as shown in Fig. 1. The x- and y-axes lay on the top surface and the x-axis is set along the fibers in the outer most layer of laminated C/Cs. Thus, the z-axis lies along the thickness direction. From now on we will use notations like 'CP-ZY'. In this notation, the 'CP' denotes the C/C type, namely CP or UD, the 'Z' specifies the coating direction (perpendicular to the z-axis) to be debonded, and the 'Y' represents the loading direction. Hereafter, the fracture experiments performed to the coating applied on the X–Y surfaces and on the Z–Y or Z–X surfaces will be referred to as top and side surface experiments, respectively.

2.3. Experimental procedure

In order to realize stable shear fracture along the interface between the coating and substrate, the test fixture made of quenched steel shown in Fig. 2 was designed and fabricated. Using this test fixture, a shear force was directly applied to the

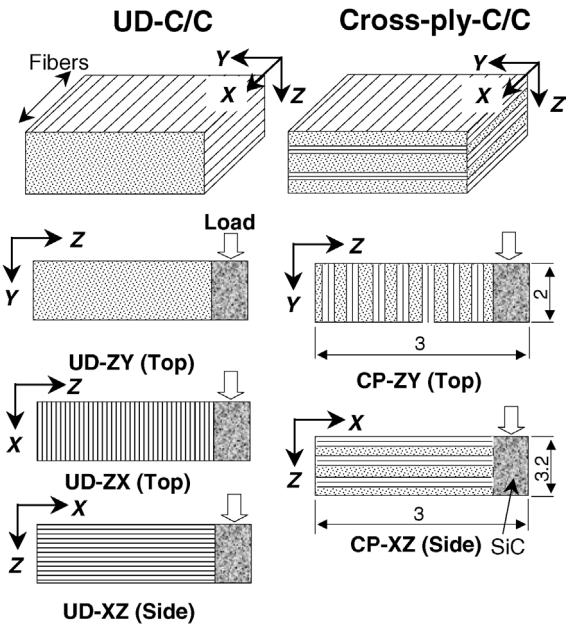

Figure 1. The notations to identify testing directions and debonding surfaces used in interfacial shear fracture tests (plunger method).

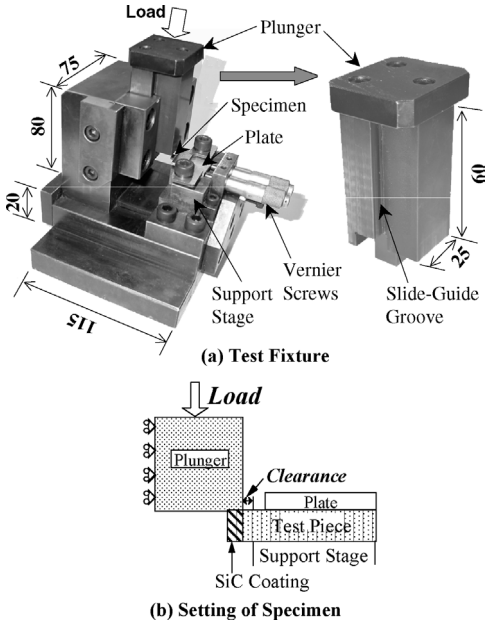

Figure 2. Schematic drawings of a test fixture to measure shear strengths of coatings (a) and specimen setting (b) for the plunger method.

coating by a near edge area of a plunger. The edge of the plunger adjacent to the loading area was carefully completed by polishing, and the edge has a curvature less than several μm. The shear loads were applied using an Instron type testing-machine under a crosshead speed of 0.01 mm/min. When the specimen was set on the support stage, the location of the coating interface was carefully arranged on enlarged views from both ends with a CCD camera and a travelling microscope. The clearance was set to 10 μm by inserting a thickness gage between the plunger and supporting stage before the tests. During the loading, crack extension was observed by the CCD camera. The dimensions of the specimens were $18 \times 3 \times 2$ mm for the top surface experiments and $18 \times 3 \times 3.2$ mm for the sides (see Fig. 1).

Bonding strengths were represented by the average shear stress obtained from the fracture loads divided by the area of the interface. Three to five tests were performed for each testing condition.

3. RESULTS

3.1. Interfacial fracture loads

Experimentally determined interfacial fracture shear stresses are plotted as a function of the coating thickness in Fig. 3. In this figure, the ordinate represents the average shear fracture stress. The plotted data are for various coatings deposited at 1200°C with a conversion time of 5 h. The observations with a CCD camera revealed that the interfacial fracture in the side surface experiments initiated from the support stage side interface and propagated in the upper direction. On the other hand in the top surface experiments, fracture initiated at the plunger side interface and propagated downward. A typical load–displacement curve is shown in Fig. 4 for a UD-XZ specimen. This figure clearly illustrates the interfacial fracture process;

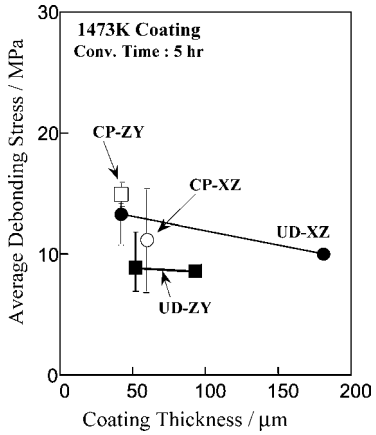

Figure 3. Averaged debonding shear stresses for various specimens as a function of coating thickness.

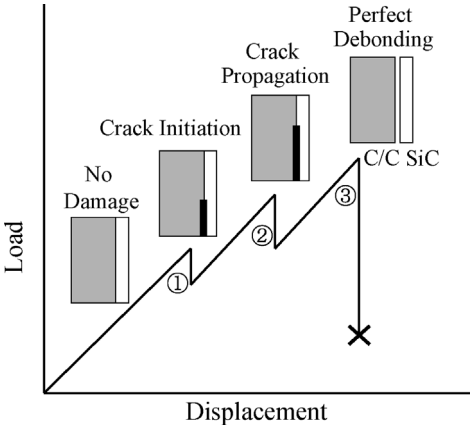

Figure 4. A typical load–displacement curve obtained by the plunger method for a UD-XZ specimen.

intermittent small drops of the load are accompanying sudden propagations of the crack.

3.2. Factors controlling interfacial fracture

The following three factors may strongly affect the interfacial strength: (1) thermal residual stress in the coating and substrate; (2) anchor effect due to penetration of coating material into transverse cracks of the substrate; and (3) duration of the conversion treatment.

The thermal strain mismatch between the SiC coating and the C/C substrate induces extremely high thermal stresses during the cooling process from the coating treatment temperature to room temperature. The thermal expansion of the C/C substrate is extremely small in fiber axis directions, and large in the thickness direction [17]. Hence in the coating, tensile stresses appear in the X- and Y-directions of the CP laminate and in the X-direction of the UD, on the other hand compressive stresses in the other directions. When coating debonds, these thermal residual stresses are partially released and the corresponding strain energy converts to surface energy. Thus, the thermal residual stress reduces fracture load of the coating interface. It is seen in Fig. 3 that the interfacial fracture stress of UD-XZ is higher than that of UD-ZY. This might be caused by the difference of thermal residual stress.

In general, C/Cs contain a large number of defects. Among them transverse cracks (TCs) are large and have significant influence on the cracking behavior of coatings. The TCs appear in laminated C/Cs due to the difference in thermal expansion between parallel and normal to fiber axis [17]. They run parallel to the fiber axis and appear periodically as through-the-ply cracks. When coating is deposited on the substrate, coating material penetrates into the TCs in the outmost plies [18]. When a load is applied to the interface, the penetrated material resists against interfacial fracture, which improves the interfacial strength. In Fig. 3, the fracture shear stress in CP-ZY is higher than that in CP-XZ. In the cross-ply laminate, the number of the

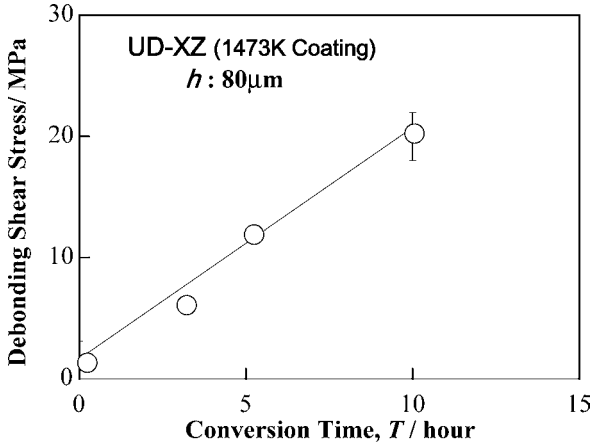

Figure 5. Averaged debonding shear stress of UD-XZ specimens as a function of conversion time.

transverse cracks in the Top surface is two times larger than that in the side surface, because TCs run in two directions in the top surface but only one direction in the side surface [19]. Thus taking the anchor effect into account, we can reasonably explain the tendency of the interfacial strengths of the CP-ZY and CP-XZ. The effect of thermal residual stress should appear in the cross-ply C/C, and this effect induces the opposite tendency shown in Fig. 3. Thus, the results for cross-ply C/Cs indicate that the effect of the anchor effect is higher than that of the thermal residual stress.

In Fig. 5, the interfacial strength of the UD-XZ is arranged as a function of conversion time. This figure clearly shows that a long conversion time improves the interfacial strength. In the conversion process, the near surface C/C reacts to form SiC. Though the detailed strengthening mechanisms of the conversion treatment are still being studied, two mechanisms can be addressed [18]. The first mechanism is again related to the anchor effect. By conversion treatment, a thin SiC layer formed near the surface of the substrate. The order of the SiC conversion is, at first, the matrix carbon near the fiber interfaces, then the matrix far from the interface, finally fibers. Thus, when the conversion time is short, only the matrix changed into SiC. This difference of penetration depth of SiC in the matrix and fiber yielded the anchor effect. The second mechanism is conversion of fiber into SiC. Then, the fiber strongly bonded to SiC coating after long conversion treatment, and the interfacial fracture tends to pass through the reinforcing fibers [18].

4. ANALYSIS

4.1. Finite element calculations

In the top surface tests, the fracture did not proceed on the interface but within the substrate. This suggests that the interfacial strength of the top surface was

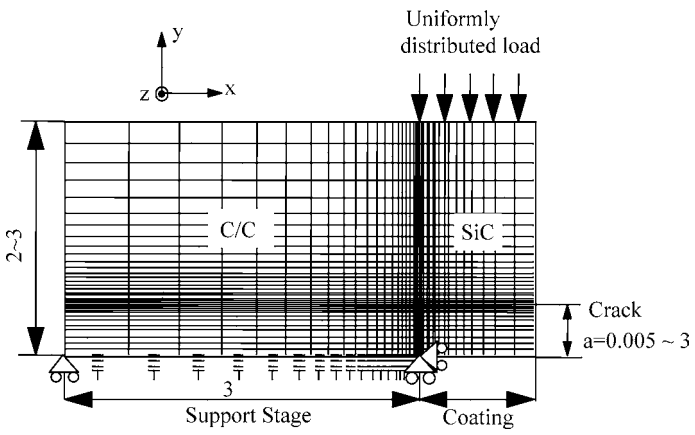

Figure 6. A finite element model for UD-XZ specimens subjected to a external load by the plunger method.

higher than the shear strength of the substrate. Since the purpose of this study is to examine the interfacial fracture of coated C/C composites, we will focus the following discussion on the UD side surface tests, in which interfacial fracture was observed.

Finite element calculations were carried out to obtain energy release rates during the interfacial fracture tests. Figure 6 shows a typical analytical model composed of 8-node quadrilateral isoparametric elements. In this model, the conversion layer was not inserted along the bonding interfaces, because the conversion layers in the present study were thin and less than several microns [18]. The finite element calculations were carried out by using a commercial code (ABAQUS) under a uniform loading condition in the contact region of the coating and plunger, i.e. no load applied in the clearance region (Fig. 2b). Energy release rates G during fracture of the interface were determined by the virtual crack-closure-force method [20, 21]. The specimens in this study were coated only on one side. Thus, during cooling from the coating treatment temperature, the specimen underwent bending deformation. In order to simulate this deformation, nonlinear spring elements were inserted between the specimen and the support stage. The springs had extremely high spring constant in the negative (compressive) direction but an extremely low one to the positive (tensile) displacement. In actual calculation, the thermal boundary condition and external load were simultaneously applied. The material properties used in the calculations were listed in Table 1.

In the calculation of G, an interfacial crack was introduced at the interface edge of the support stage side in accordance with experimental observations. This tendency was reconfirmed by calculation; Gs in the side experiment were compared for the cracks extending from the support stage side and from the plunger side under constant load. The results confirmed that G is much higher in the former than in the latter case.

Table 1.
Material properties used in FEM calculations for interfacial debonding process of SiC coated C/C composites.

Materials	Young's modulus (GPa)		Shear modulus (GPa)	Poisson's ratio			CTE (ppm/K) at 1473 K	
	E_{zz}	E_{yy}	G_{xz}	ν_{xy}	ν_{yz}	ν_{zx}	α_z	α_y
CP-C/C	90	15	7	0.1,	0.01,	0.4	0.15	9.0
UD-C/C	180	15	7	0.3,	0.01,	0.4	0.15	9.0
SiC	490		—		0.25		4.9	

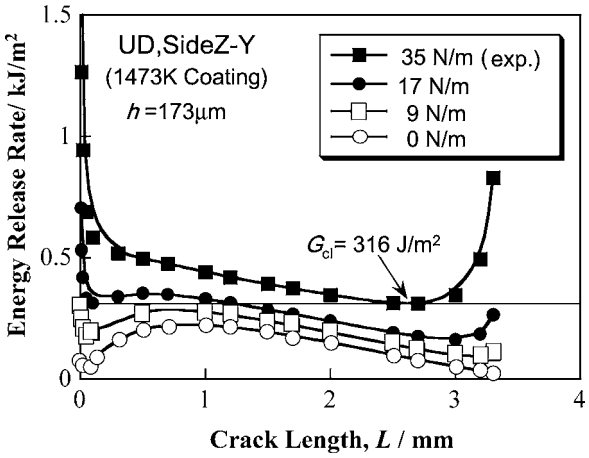

Figure 7. Energy release rates as a function of crack length, L.

The calculated energy release rates for various loads are shown in Fig. 7 as a function of the crack length under the assumption of a coating thickness of 173 μm. In this case, the coating interface ultimately fractured at an external load of 35 N/m. On the 35 N/m curve shown in Fig. 7, G attains the minimum at a crack length of 2.7 mm. This clearly indicates that the crack is stable up to a crack length of 2.7 mm but becomes unstable after that, which agrees well with experimental observations. The critical energy release rate G_c corresponds to the onset of unstable crack growth. Thus from Fig. 7, G_c for the coating with conversion treatment for 5 h was found to be 316 J/m^2.

4.2. Prediction of fracture load

Using the determined G_c, the interfacial fracture loads were predicted for coatings with various thicknesses and coating treatment temperatures. These predictions were made under the assumptions that coating treatment temperature and coating thickness affected bonding strength of SiC coating only by thermal residual stress. As a reference bonding strength, we used bonding strength of 1200°C coating

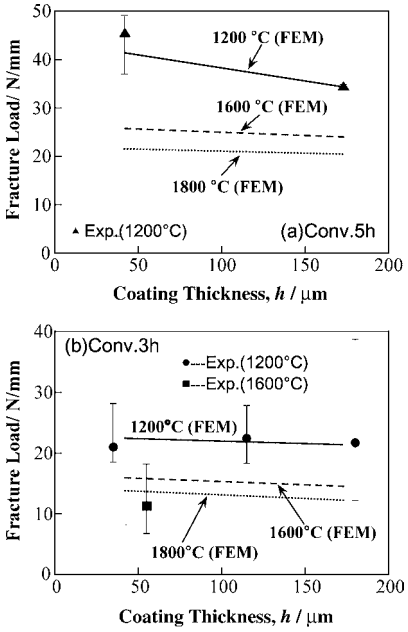

Figure 8. Prediction of interfacial fracture loads for UD-XZ specimens having various coating thicknesses and coated at various temperatures. (a) 5 h conversion, (b) 3 h conversion.

with a thickness of 180 μm, in other words $G_c = 316$ J/m^2. Figures 8a and 8b demonstrate the calculation results for conversion times of 3 and 5 h, respectively. As shown in these figures, the experimental results agree reasonably well with analytical predictions. Thus, it can be concluded that the G-criterion is effective for the interfacial fracture evaluation. It is also seen in these figures that the fracture load increased with decreasing coating thickness and coating treatment temperature.

4.3. Delamination in the C/C substrate

The coating cracks on the Top surface of the UD C/C penetrated into the substrate and then propagated parallel to the coating surface as shown in Fig. 9a, though the parallel crack was slight in the thinner coating shown in Fig. 9b. So far, we have mainly discussed the coatings deposited on the side surface, in which cracks have propagated parallel to the loading direction. Thus the influence of the coating cracks on the interfacial strength of coatings could be neglected. On the other hand, in the coatings on the top surface of C/Cs, the cracks are considered to have significant effects. Thus to substantiate these defects, let us define the crack spacing, the distance between neighbouring cracks 2λ, the crack penetration depth D_s, and the debonding length L_d as shown in Fig. 10. Figures 11a to 11c show distributions of 2λ, D_s, and L_d for coatings applied at 1200°C. As shown in these figures, 2λ, D_s, and L_d increase with coating thickness, and the substrate delaminations in a thin coating are quite small.

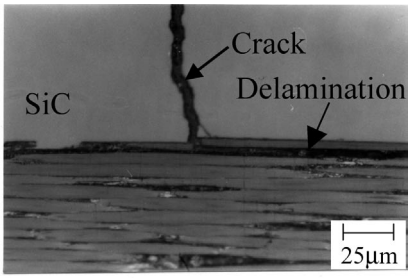

(a) Coating Thickness: 173 μm

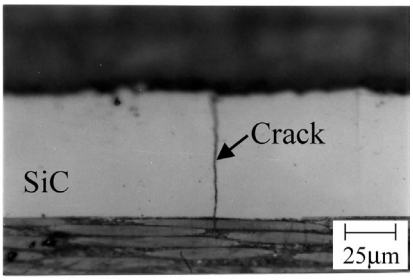

(b) Coating Thickness: 62 μm

Figure 9. Optical microphotographs of cross-sections of SiC-coated C/C composite when coating thicknesses, hs, were (a) 173 μm and (b) 62 μm.

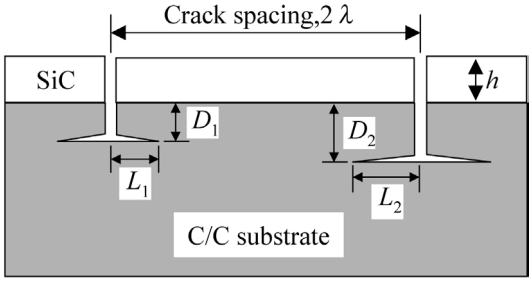

Averaged crack penetration depth, $D_s = (D_1+D_2)/2$

Averaged delamination length, $L_d = (L_1+L_2)/2$

Figure 10. Schematic drawing for the definition of crack spacing 2λ, crack penetration depth D_s, and delamination length L_d.

To analyze the substrate delamination, finite element calculations were carried out. Figure 12 shows a finite element mesh for the delamination analysis of the coating. Like the discussions for the UD side surface, 8-node quadrilateral isoparametric elements were used and the virtual crack closure method was adopted to determine the energy release rates. The analyses were performed for coating

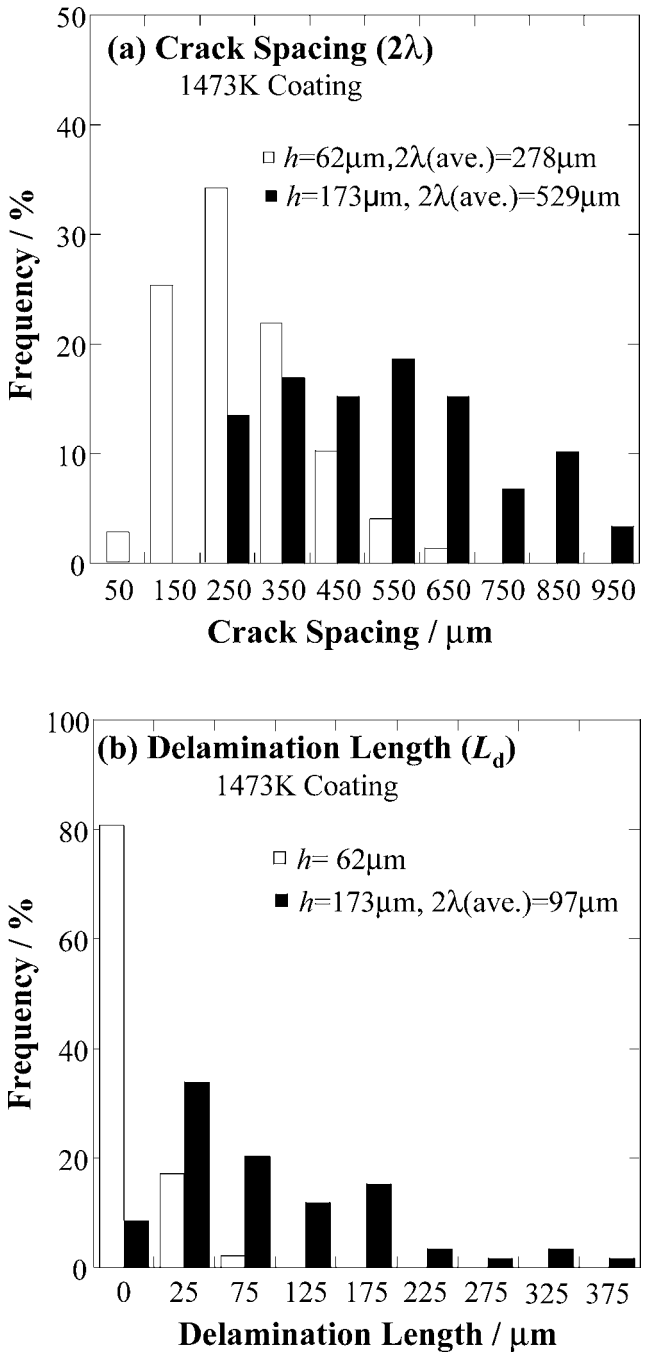

Figure 11. Distributions of (a) crack spacing 2λ, (b) delamination length D_s, and (c) crack penetration depth L_d for UD-ZX specimens.

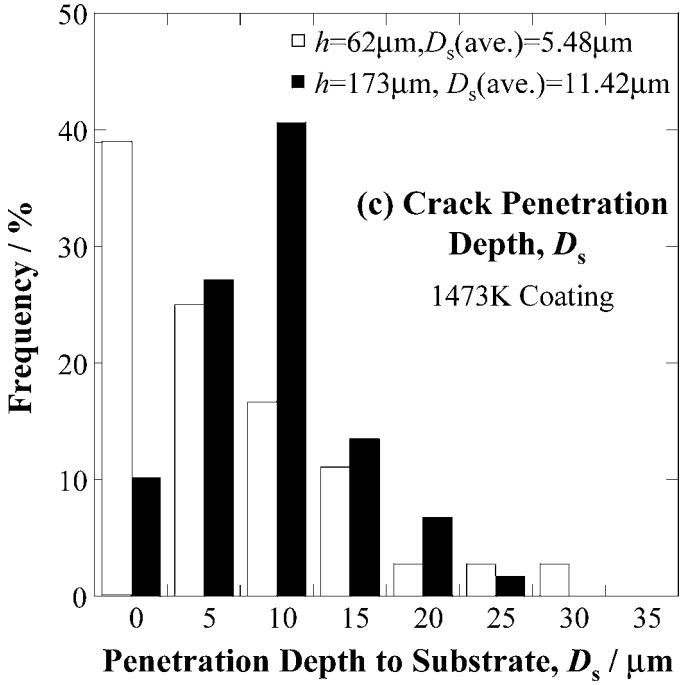

Figure 11. (Continued).

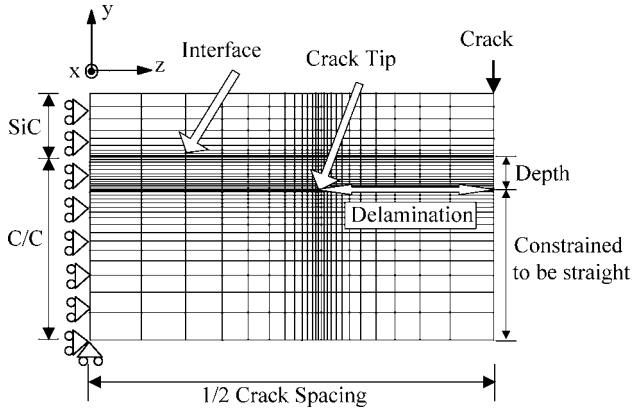

Figure 12. A finite element model for analyses of interfacial delamination of UD-ZX specimens under thermal loading.

thicknesses of 173 and 62 μm. The half distance of the spacing was modeled under the assumption that crack spacing and penetration depth are constant and equal to the average values.

Figure 13 shows calculated energy release rates as a function of the delamination length along the interface when the specimen is subjected to temperature drop

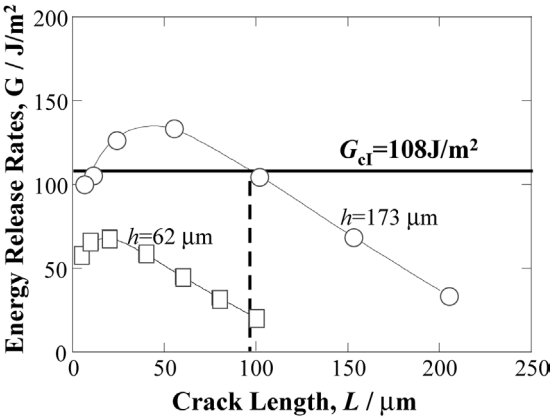

Figure 13. Comparison of G_c with G during debonding extension along the coating/substrate interfaces for two coatings having different thicknesses, hs, as a function of crack length, L.

from 1200°C to room temperature. For the 173 μm coating, the measured average delamination length was 97 μm. Hence the energy release rate G at this point should be the critical value G_c. Under this assumption, we can estimate G_c to be 108 J/m^2. When the crack length is extremely small, however, a value of G smaller than 108 J/m^2 was obtained. This low G can be understood if it can be assumed that the defects, whose dimension was larger than this crack length, existed in the substrate. The curve for the 62 μm coating is lower than G_c, which indicates no delaminations. In fact, no delaminations were observed for 80% of coating cracks for this case.

To confirm the adequacy of the above obtained G_c, the delamination on the Top surface of the UD C/C was further extended by interfacial loading using the plunger method. Then, G during crack extension was calculated using the finite element model shown in Fig. 14. This model includes four crack spacings, which is consistent with the actual specimens, and both the thermal stresses and the external force were taken into consideration. By comparison of Gs for the crack extensions of individual cracks, it was found that G was maximum when the crack extended from the top interface of the model. The experiments were performed for the 173 μm coating. Figure 15 illustrates calculation results for three loading conditions. In this figure the calculation results corresponding to the full, a half, and zero external loads are also shown to demonstrate the effect of the external load. The energy release rate assuming no external load is different from that in Fig. 13. This happened due to stress relaxation during processing specimens into the small size, but not due to damage during the cutting. The fully loaded solid line increases with crack length. This curve indicates that the fracture was unstable and the fracture load was governed by the initial G value. Note that the initial value agrees well with the estimated G_c, 108 J/m^2.

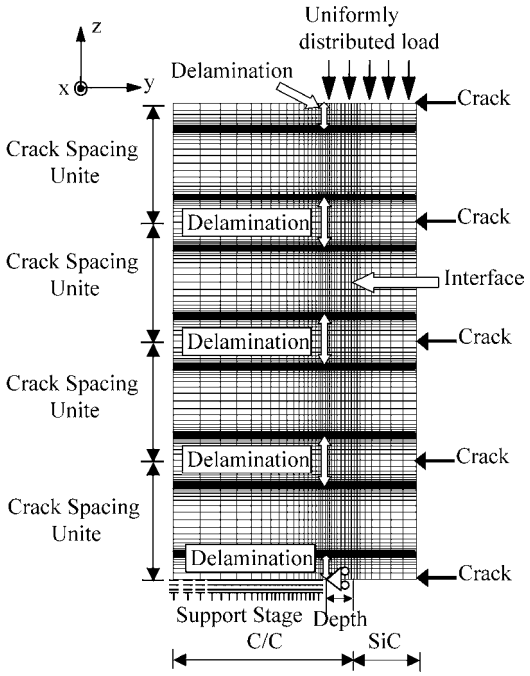

Figure 14. A finite element model for interfacial delamination of UD-ZX specimens under thermal and external loading.

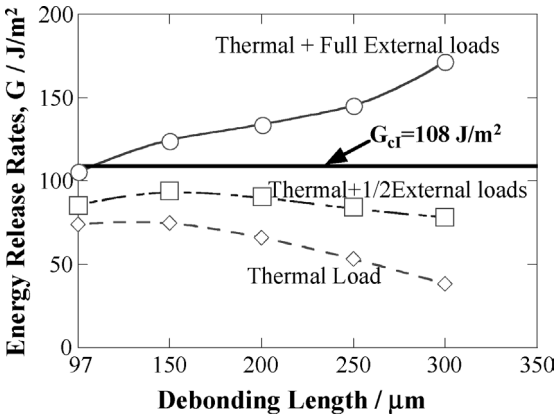

Figure 15. Energy release rates for UD-ZX specimens under thermal and external loading as a function of debonding length of SiC coating.

5. CONCLUSION

As an evaluation technique for the interfacial bonding strength between a SiC coating and a C/C substrate, a plunger method was proposed in this paper. To quantify the measured results, the critical energy release rates were determined using the finite element method for various coated C/C composites. Through

comparison of the experimental and calculation results, the following conclusions were reached.

(1) The plunger method is a quite effective evaluation technique for the measurement of the interfacial bonding, in particular, for that with small dimension specimens.

(2) The prediction of the interfacial fracture can be made by use of the critical energy release rate of the interface, which can be obtained by finite element calculations.

(3) The interfacial bonding was predicted to be stronger when the coating treatment temperature was lowered and the coating was thinner.

Acknowledgement

This work was financially supported in part by Grant-in-Aids for Scientific Research (No. 09555202) from the Japanese Ministry of Education, Science, Sports, and Culture.

REFERENCES

1. J. D. Buckley, Carbon-Carbon Materials and Composites, 12, *NASA Reference Publication* 1254 (1992).
2. E. Fitzer, A. Gkogkidis and M. Heine, Carbon fibers and their composites (a review), *High Temperatures High Pressures* **16** (9), 363 (1984).
3. D. W. McKee, *Carbon* **17**, 551 (1987).
4. J. E. Sheehan, *Carbon* **27**, 709 (1989).
5. ASTM D 897.
6. JIS R4204-1963, JIS H8666-1990 and JIS K5400-1990.
7. T. Tanaka, in: *Properties and Evaluations of Coatings*, p. 199. Riko Shuppan Co., Japan (1993) (in Japanese).
8. K. Nakasa and S. Takata, *J. Japan Soc. Mater. Sci.* **44**, 321 (1995).
9. K. Nakasa and M. Kato, *J. Japan Soc. Mater. Sci.* **45**, 680 (1996).
10. M. Kato and K. Nakasa, *J. Japan Soc. Mater. Sci.* **46**, 315 (1997).
11. A. G. Evans and J. W. Hutchinson, *Intern. J. Solids Struct.* **20**, 455 (1984).
12. D. B. Marshall and A. G. Evans, *J. Appl. Phys.* **56**, 2632 (1984).
13. D. B. Marshall and A. G. Evans, *J. Appl. Phys.* **56**, 2639 (1984).
14. Y. Kogo, H. Hatta and A. Okura, *Trans. Tokyo Polytechnic Institute* **17**, 50 (1994).
15. T. Aoki, H. Hatta, Y. Kogo, H. Fukuda, T. Goto and T. Yarii, *J. Japan Inst. Metal* **62**, 4 (1998).
16. H. Hatta, Y. Kogo, Y. Osawa and I. Shiota, Interfacial strength between SiC coatings and C/C composites, in: *Ceramic Transactions, Vol. 99, Ceramic Material Systems with Composite Structures*, pp. 149–156 (1998).
17. H. Hatta, Y. Kogo, Y. Yoshihara, Y. Sawada, K. Takahashi, K. Hosono and T. Dozono, *Materials Systems* **14**, 15–24 (1995).
18. H. Hatta, D. Maruyama and Y. Kogo, *Material Systems* **22**, 59 (2004).
19. H. Hatta, T. Aoki, Y. Kogo and T. Yarii, *Composites*, *Part A* **30**, 515–520 (1999).
20. E. F. Rybicki and M. F. Kanninnen, *Engng. Fracture Mech.* **9**, 931 (1977).
21. K. N. Shivakumar, P. W. Tan and J. C. Newman, *Intern. J. Fracture* **36** (1988).